European Commission

JRC TECHNICAL REPORTS

Recommendations for the neutron cross section standards project

Description of GELINA data recommended for a new neutron standards evaluation

Franz-Josef Hambsch
Stefan Kopecky
Markus Nyman
Adina Olacel
Carlos Paradela

2016

Joint Research Centre

EUR 28161 EN

This publication is a Technical report by the Joint Research Centre, the European Commission's in-house science service. It aims to provide evidence-based scientific support to the European policy-making process. The scientific output expressed does not imply a policy position of the European Commission. Neither the European Commission nor any person acting on behalf of the Commission is responsible for the use which might be made of this publication.

JRC Science Hub
https://ec.europa.eu/jrc

JRC103456

EUR 28161 EN

ISBN 978-92-79-62864-1

ISSN 1831-9424

doi:10.2789/306587

How to cite: F.-J. Hambsch, S. Kopecky, M. Nyman, A. Olacel and C. Paradela; Recommendations for the neutron cross section standards project ; EUR 28161 EN; doi:10.2789/306587

JRC recommendations for neutron cross section standards project

F.-J. Hambsch[a], S. Kopecky[a], M. Nyman[a], A. Olacel[a,b] and C. Paradela[a]

[a]European Commission, Joint Research Centre, B - 2440 Geel, Belgium

[b]Horia Hulubei National Institute for Physics and Nuclear Engineering, Reactorului 30, 077125 Bucharest-Măgurele, Romania

Contents

Abstract 2
1 Introduction 3
2 Data for the $^{10}B(n,\alpha_0)$ and $^{10}B(n,\alpha_1)$ reactions 4
3 Average capture cross section data 6
3.1 Average capture cross section data for $^{197}Au(n,\gamma)$ 7
3.2 Average capture cross section data for $^{238}U(n,\gamma)$ 8
4 Gamma-ray production cross section data 9
4.1 Cross section data for $^{7}Li(n,n'\gamma)$ 9
4.2 Cross section data for $^{48}Ti(n,n'\gamma)$ 10
5 Conclusion 12
References 13
List of abbreviations and definitions 15
List of figures 16
List of tables 17

Abstract

This report describes cross section data for the ^{7}Li(n,n'γ), ^{10}B(n,α_0), ^{10}B(n,α_1), ^{48}Ti(n,n'γ), ^{197}Au(n,γ) and ^{238}U(n,γ) reactions, which were obtained from measurements at the GELINA facility installed at the JRC Geel. The data are recommended for a new evaluation of neutron cross section standards organised by the Nuclear Data Section of the IAEA. The Legendre polynomials for the angular differential cross section of ^{10}B(n,α_0) and ^{10}B(n,α_1) are tabulated. The average cross sections for the ^{238}U(n,γ) and ^{197}Au(n,γ) reactions together with their full covariance information have been formatted such that they can directly be stored in the EXFOR data library.

1 Introduction

Neutron cross seciton standards are the basis for the determination of most of the cross sections for neutron induced reactions. In response to requests for improvements in the neutron standards, the Cross Section Evaluation Working Group (CSEWG), the Working Party on International Evaluation Cooperation (WPEC) of the Nuclear Energy Agency Nuclear Science Committee and the International Atomic Energy Agency (IAEA) are working cooperatively to provide new evaluations of the standards [1]. An international effort at several IAEA technical meetings made important contributions to the evaluation process [2].

The need to re-evaluate the neutron cross section standards is based on the appearance of a substantial amount of accurate new experimental data and improved developments in the methodology of analysis and evaluation. The cross sections being evaluated are those for the H(n,n), ^{6}Li(n,t), ^{10}B(n,$\alpha_1\gamma$), ^{10}B(n,α), C(n,n), ^{197}Au(n,γ), ^{235}U(n,f) and ^{238}U(n,f) reactions. Also included in the evaluation process are the ^{238}U(n,γ) and ^{239}Pu(n,f) reaction cross sections. In addition, the present standards project includes an evaluation of thermal constants, of reference cross sections for neutron induced γ-ray production cross sections, high energy fission cross sections and prompt fission neutron spectra.

In this report the contribution of the JRC Geel to the standards project is summarised. More in particular, it describes cross section data produced at GELINA that will be included in the new standards evaluation process.

2 Data for the $^{10}B(n,\alpha_0)$ and $^{10}B(n,\alpha_1)$ reactions

R. Bevilacqua*, F.J. Hambsch, I. Ruskov** and M. Vidali
*European Spallation Source ERIC, Lund, Sweden
**Institute for Nuclear Research and Nuclear Energy, Sofia, Bulgaria

The $^{10}B(n,\alpha_0)$ and $^{10}B(n,\alpha_1\gamma)$ angular distributions have been measured at the GELINA time-of-flight (TOF) spectrometer [3] in the incident neutron energy range from 0.1 MeV to 1 MeV. The experimental setup is described in detail in Ref. [4]. This report describes the most important aspects. Two different flight-path distances from the GELINA neutron producing target were used: L1 ~28.24 m using a moderated beam and L2 ~57.41 m using an un-moderated beam. In-beam filters of Bi and Pb were used to reduce the gamma flash from the neutron production. The capture and scattering resonances in those materials served as an intrinsic energy calibration of the TOF- spectra.

A twin Frisch-grid ionization chamber (TFGIC) was used to detect the $^{10}B(n,\alpha)^7Li$ reaction products. The chamber was loaded with two thin ^{10}B-samples mounted back-to-back at the common cathode. The boron samples, enriched to 94% in ^{10}B, had an areal density of (14.5 +/- 0.8) μcm^2 and (15.7 +/- 0.8) $\mu g/cm^2$, respectively, a diameter of 84 mm and were vacuum evaporated on a polished tantalum backing of 0.3 mm thickness and 100 mm diameter. The angular distribution was measured in a close to 2 x 2π solid angle geometry, with a clear separation of the two reaction channels: emission to the ground state (α_0) and first excited state (α_1). A coverage of nearly the full solid angle was achieved at incident neutron energies from 100 keV up to 1 MeV. The parameters of the Legendre polynomial fitted to the angular distributions are given in Table 1 and Table 2. These data will be taken up in the new standards evaluation.

E_n / keV	u_{En} / keV	A_0	u_{A0}	A_1/A_0	$u_{A1/A0}$	A_2/A_0	$u_{A2/A0}$	A_3/A_0	$u_{A3/A0}$
0.15	-	247.19	1.66	-0.02718	0.01179	-0.04129	0.01939	0.00391	0.02055
0.7	0.3	159.83	1.33	-0.0448	0.01459	0.01993	0.02409	-0.02698	0.02544
1.5	0.5	87.82	1.04	0.03821	0.02085	-0.01447	0.03436	0.04738	0.03636
2.5	0.5	48.80	0.72	0.07714	0.02585	-0.02843	0.04253	0.02115	0.04503
4.0	1.0	61.55	1.03	0.01502	0.02944	0.05760	0.04872	-0.05341	0.05133
7.5	2.5	75.73	0.96	0.01682	0.02224	-0.08734	0.03651	-0.04411	0.03878
15	5.0	62.38	0.94	0.0967	0.02651	-0.10287	0.04343	-0.02505	0.04616
30	10	57.86	0.81	0.12192	0.02459	-0.02859	0.04041	0.05511	0.04279
44.6	4.0	10.70	0.34	0.08113	0.05628	-0.22881	0.09179	0.17297	0.09818
54.57	6.0	14.06	0.42	0.22039	0.05342	-0.06543	0.08713	0.16759	0.09257
80	20	32.92	0.61	0.22958	0.03283	-0.09013	0.05344	-0.09422	0.05679
120	20	29.14	0.54	0.20976	0.03271	-0.05135	0.05343	-0.0508	0.05665
159.9	20	29.52	0.55	0.12283	0.0328	0.18109	0.05464	-0.15725	0.05713
200	20	32.80	0.64	-0.02903	0.03418	0.19236	0.05711	-0.14039	0.05965
240.3	20	34.31	0.71	-0.09732	0.0362	0.11734	0.06007	0.11711	0.06307
280.2	20	32.31	0.74	-0.21396	0.03965	0.09146	0.0653	0.04565	0.06864
320	20	35.40	0.63	-0.26022	0.03134	0.04313	0.05128	-0.02689	0.05406
360.3	20	30.96	0.61	-0.42825	0.0356	0.02755	0.05715	0.07639	0.06033
399.8	20	35.96	0.74	-0.51124	0.03769	0.15994	0.06034	-0.03687	0.06311
440.3	20	38.71	0.72	-0.51914	0.03404	0.09837	0.05418	-0.00862	0.05692
480.6	20	45.28	0.73	-0.41653	0.0289	0.18384	0.04698	0.05111	0.04905
519.5	20	54.79	0.85	-0.56304	0.02877	0.16856	0.04571	0.12217	0.04781
559.8	20	33.02	0.61	-0.48725	0.03394	0.18076	0.05461	0.13658	0.05708
599.8	20	28.19	0.59	-0.40807	0.03772	0.29839	0.06195	0.13828	0.06413
639.7	20	20.85	0.54	-0.42467	0.04712	0.15692	0.07635	0.0956	0.07991
679.5	20	18.59	0.45	-0.26137	0.04154	0.13884	0.0684	-0.02491	0.07165
720.8	20	18.16	0.49	-0.36971	0.04811	0.11207	0.07822	0.00834	0.0821
760.9	20	14.52	0.41	-0.18663	0.04982	-0.05178	0.08149	0.08606	0.08642
801.4	20	16.23	0.42	-0.17570	0.04581	-0.00103	0.07519	-0.02815	0.07949
839.3	20	13.16	0.40	-0.28129	0.05449	0.05583	0.08905	0.14469	0.09392
879.9	20	10.51	0.37	-0.07309	0.06124	0.13784	0.10184	0.06787	0.10671
920.1	20	11.01	0.38	-0.11907	0.06126	0.16468	0.10193	0.03539	0.10658
959.4	20	9.99	0.34	-0.07559	0.05876	0.07922	0.09732	0.1951	0.10258

Table 1 Parameters of the Legendre polynomials for the α_0 channel.

E_n / keV	u_{En} / keV	A_0	u_{A0}	A_1/A_0	$u_{A1/A0}$	A_2/A_0	$u_{A2/A0}$	A_3/A_0	$u_{A3/A0}$
0.15	--	3791.60	7.29	-0.00037	0.00338	-0.02376	0.00557	-0.01111	0.00589
0.7	0.3	2487.60	5.79	-0.00589	0.00409	-0.01593	0.00675	0.02242	0.00714
1.5	0.5	1357.28	3.79	-0.00283	0.00491	-0.00967	0.00809	-0.02005	0.00856
2.5	0.5	750.01	3.06	0.00271	0.00716	-0.00288	0.01182	-0.0031	0.01249
4	1.0	931.98	3.43	0.01437	0.00653	-0.00437	0.01065	-0.02792	0.01135
7.5	2.5	1185.58	3.79	0.04390	0.00563	-0.02958	0.00927	-4.6E-4	0.00981
15	5.0	1010.39	3.78	0.06740	0.00658	-0.02121	0.01083	-0.04285	0.01147
30	10	912.30	3.63	0.02951	0.00699	-0.03226	0.0115	-0.02307	0.01218
44.6	4.0	158.78	1.42	0.03338	0.01577	-0.08078	0.02591	2.5E-4	0.02750
54.57	6.0	214.78	1.55	0.07255	0.01273	-0.05732	0.02091	-0.05347	0.02218
80	20	490.49	2.46	0.04047	0.00882	-0.04505	0.01451	0.04135	0.01538
120	20	382.40	2.21	0.05576	0.01017	-0.01061	0.01676	0.04179	0.01773
159.9	20	334.32	2.08	0.08049	0.01092	-0.00785	0.01799	0.02109	0.01902
200	20	310.54	1.75	0.09975	0.00994	-0.00305	0.01637	0.00432	0.01731
240.3	20	259.69	1.83	0.14602	0.01241	-0.00431	0.02039	0.00213	0.02156
280.2	20	220.95	1.70	0.17384	0.01356	-0.01935	0.02223	-0.02148	0.02353
320	20	217.00	1.56	0.24421	0.01273	-0.01781	0.02078	-0.06242	0.02199
360.3	20	163.32	1.30	0.29671	0.01422	0.01848	0.02316	0.02870	0.02445
399.8	20	168.33	1.48	0.50106	0.01607	0.06795	0.0256	-0.0564	0.02695
440.3	20	149.62	1.43	0.72530	0.01822	0.03309	0.02783	-0.05411	0.02937
480.6	20	153.84	1.44	0.99799	0.01899	0.12353	0.02746	-0.0825	0.02880
519.5	20	144.29	1.45	0.99815	0.02035	0.09953	0.02937	0.0479	0.03086
559.8	20	81.74	0.99	1.13229	0.02538	0.17479	0.03561	-0.22555	0.03730
599.8	20	69.64	0.87	0.89139	0.02477	0.06854	0.0366	-0.01345	0.03852
639.7	20	50.27	0.83	0.88425	0.03254	0.05392	0.04811	-0.01971	0.05069
679.5	20	44.28	0.82	0.85446	0.03602	0.07355	0.05368	-0.00287	0.05649
720.8	20	36.87	0.68	0.63977	0.03468	0.09028	0.05406	-0.03461	0.05682
760.9	20	31.09	0.62	0.71767	0.0377	0.11003	0.05798	-0.06631	0.06087
801.4	20	31.32	0.61	0.69011	0.03685	0.20074	0.05736	0.07041	0.05982
839.3	20	21.40	0.46	0.60165	0.04025	0.03418	0.06294	0.20876	0.06655
879.9	20	18.31	0.49	0.59054	0.04994	0.14651	0.07885	-0.04655	0.08256
920.1	20	16.71	0.43	0.61434	0.04756	0.16769	0.07489	-0.04008	0.07829
959.4	20	13.97	0.43	0.44745	0.05646	0.12066	0.09095	0.07225	0.09543

Table 2 Parameters of the Legendre polynomials for the α_1 channel

3 Average capture cross section data

Capture cross section measurements have been performed at the time-of-flight facility GELINA [3] to determine the average capture cross section for ^{197}Au and ^{238}U in the unresolved resonance region. The procedures described in Ref. [5] were followed. A detailed description of the experiments is given in Refs. [6] and [7] for the $^{197}Au(n,\gamma)$ and $^{238}U(n,\gamma)$ reaction, respectively.

The total energy detection principle combined with the pulse height weighting technique was applied [5]. The energy dependence of the neutron flux was measured with ionisation chambers based on the $^{10}B(n,\alpha)$ reaction. The impact of kinematic effects for the flux measurements was strongly reduced by using multiple chambers with a common cathode loaded with two layers of ^{10}B. Such a back-to-back configuration together with a low energy threshold on the amplitude spectrum accepting the signals from both the ^{7}Li and α particles strongly reduces a possible bias related to the forward-to-backward emission ratio [8]. The data were internally normalised to an isolated and saturated resonance profile.

The capture detection systems (i.e. γ-ray detectors, neutron flux detector, electronics and data acquisition system) for all measurements were very similar. Prompt γ-rays originating from a capture reaction were detected by a set of C_6D_6-based liquid scintillators (NE230) of 10 cm diameter and 7.5 cm length. The detection of neutrons scattered from the sample was reduced by coupling each scintillator to a boron-free quartz windowed EMI9823-KQB photomultiplier (PMT).

Permanent black resonance filters (Na and/or S) were used to monitor the background and reduce bias effects related to background corrections. Due to the use of a Na background filter the data in the energy region between 2.5 keV and 3.5 keV cannot be analysed, while the use of a S filter restricts the analysis of the data to an upper level of 90 keV.

Measurements with different sample geometries and thickness and with different fixed black resonance filter configurations were carried out to reduce systematic effects related to background corrections and to the sample geometry and thickness, i.e. correction for γ-ray transport in the sample and corrections for self-shielding and multiple interaction events.

To derive the average cross sections and propagate both the correlated and uncorrelated uncertainties the AGS code was used. Applying the AGS concept described in Ref. [9], the covariance matrix V can be calculated by:

$$V = U_u + S\,S^T,$$

where U_u is a diagonal matrix containing the contribution of all uncorrelated uncertainty components. The matrix S contains the contribution of the components creating correlated components.

3.1 Average capture cross section data for ^{197}Au(n,γ)

J.C. Drohe, C. Massimi*, P. Schillebeeckx and R. Wynants
*INFN Bologna, Via Irnerio 46, I – 40126 Bologna

Capture cross section measurements have been carried out at a 12.5 m and 30 m station of GELINA using a 0.5 mm and 1.0 mm thick metallic gold disc. Details about the experiments and data reduction can be found in Ref. [6]. The data have been normalized to the saturated resonance profile at 4.9 eV. The data obtained with the 1.0 mm sample was used to validate the correction for self-shielding and multiple interaction events, while the 30 m data were used to verify the impact of the flight path distance. The resulting average capture cross section together with the covariance data in AGS format are listed in Table 3. The data in Table 3 include the contribution to the covariance data due to uncorrelated uncertainties from counting statistics (u_u) and the correlated components due to the background in the capture system (S_{b0},S_{k1},S_{k2}) and the normalization S_{Nc}. The correlated components due to the time independent background, the time dependent and time and sample dependent component are represented by S_{b0}, S_{k1} and S_{k2}, respectively. The main uncertainty component is due to the normalization.

E_l	E_h	σ_γ	$u_{\sigma\gamma}$	AGS				
				u_u	S_{b0}	S_{k1}	S_{k2}	S_{Nc}
3500	4000	2.8696	0.0354	0.0084	-0.001731	-0.012957	-0.004330	0.031566
4000	4500	2.2833	0.0284	0.0070	-0.001352	-0.010596	-0.003448	0.025116
4500	5000	2.0888	0.0251	0.0058	-0.000981	-0.007942	-0.002375	0.022977
5000	5500	1.5480	0.019	0.0047	-0.000803	-0.006683	-0.001828	0.017028
5500	6000	2.1886	0.0259	0.0057	-0.000734	-0.006767	-0.003384	0.024075
6000	6500	1.7350	0.0207	0.0051	-0.000649	-0.006058	-0.001689	0.019085
6500	7000	1.7219	0.0204	0.0049	-0.000567	-0.005428	-0.001737	0.018941
7000	8000	1.5664	0.0184	0.0036	-0.000554	-0.005162	-0.001519	0.017230
8000	9000	1.3120	0.0156	0.0034	-0.000494	-0.004555	-0.001419	0.014432
9000	10000	1.1502	0.0137	0.0032	-0.000437	-0.004116	-0.001166	0.012652
10000	12000	1.1625	0.0135	0.0023	-0.000374	-0.003588	-0.001109	0.012788
12000	14000	0.9572	0.0113	0.0022	-0.000324	-0.003234	-0.000963	0.010529
14000	16000	0.8569	0.0102	0.0022	-0.000283	-0.002963	-0.000830	0.009426
16000	18000	0.8215	0.0097	0.0022	-0.000250	-0.002674	-0.000756	0.009037
18000	20000	0.7329	0.0087	0.0021	-0.000225	-0.002411	-0.000705	0.008062
20000	24000	0.6418	0.0076	0.0015	-0.000195	-0.002145	-0.000650	0.007060
24000	28000	0.6165	0.0072	0.0015	-0.000168	-0.001929	-0.000703	0.006781
28000	32000	0.5842	0.0076	0.0026	-0.000242	-0.002914	-0.000896	0.006426
32000	36000	0.5160	0.0062	0.0016	-0.000144	-0.001835	-0.000669	0.005676
36000	40000	0.5168	0.0061	0.0015	-0.000122	-0.001581	-0.000575	0.005685
40000	44000	0.4709	0.0056	0.0014	-0.000103	-0.001343	-0.000487	0.005180
44000	52000	0.4403	0.0051	0.0010	-0.000089	-0.001119	-0.000440	0.004843
52000	60000	0.4192	0.0049	0.0011	-0.000088	-0.001074	-0.000610	0.004612
60000	68000	0.3894	0.0045	0.0009	-0.000062	-0.000739	-0.000523	0.004284
68000	76000	0.3771	0.0043	0.0009	-0.000054	-0.000632	-0.000500	0.004148
76000	84000	0.3429	0.0039	0.0009	-0.000054	-0.000619	-0.000335	0.003772

Table 3 Average capture cross section for ^{197}Au(n.γ) together with the full covariance information based on the AGS concept.

3.2 Average capture cross section data for $^{238}U(n,\gamma)$

H.I. Kim*, G. Alaerts, S. Kopecky, A. Moens, C. Paradela, P. Schillebeeckx, R. Wynants
*Korea Atomic Energy Research Institute, Daejeon 34057, Republic of Korea

Capture cross section measurements have been carried out at a 12.5 m and 60 m station of GELINA using two different sample configurations with a thickness of about 0.23 and 0.46 mm and with different fixed black resonance filter configurations. The data have been normalized to the saturated resonance profile at 6.67 eV. Details about the experiments and data reduction can be found in Ref. [7]. The resulting average capture cross section together with the full covariance information in AGS format are listed in Table 4. The data include the contribution to the covariance data due to uncorrelated uncertainties from counting statistics (u_u) and the correlated components due to the background in the capture system S_k and the normalization S_{Nc}.

E_l / eV	E_h / eV	σ_γ / b	$u_{\sigma\gamma}$ / b	AGS		
				u_u	S_{Nc}	S_k
3500	4000	0.9828	0.0340	0.0138	0.0147	-0.0273
4000	4500	0.8645	0.0246	0.0092	0.0130	-0.0188
4500	5000	0.9743	0.0234	0.0085	0.0146	-0.0162
5000	5500	0.8448	0.0209	0.0080	0.0127	-0.0146
5500	6000	0.9355	0.0220	0.0088	0.0140	-0.0145
6000	6500	0.9226	0.0212	0.0087	0.0138	-0.0135
6500	7000	0.8286	0.0198	0.0085	0.0124	-0.0129
7000	8000	0.7726	0.0174	0.0058	0.0116	-0.0116
8000	9000	0.6521	0.0153	0.0056	0.0098	-0.0104
9000	10000	0.6958	0.0152	0.0054	0.0104	-0.0096
10000	12000	0.6657	0.0138	0.0039	0.0100	-0.0087
12000	14000	0.6458	0.0132	0.0040	0.0097	-0.0079
14000	16000	0.5860	0.0120	0.0040	0.0088	-0.0071
16000	18000	0.5787	0.0117	0.0040	0.0087	-0.0067
18000	20000	0.5366	0.0108	0.0039	0.0081	-0.0060
20000	22500	0.5246	0.0103	0.0035	0.0079	-0.0056
22500	25000	0.4871	0.0095	0.0033	0.0073	-0.0050
25000	27500	0.4608	0.0090	0.0033	0.0069	-0.0048
27500	30000	0.4453	0.0089	0.0035	0.0067	-0.0047
30000	35000	0.4230	0.0088	0.0031	0.0064	-0.0052
35000	40000	0.3942	0.0077	0.0026	0.0059	-0.0042
40000	45000	0.3767	0.0069	0.0022	0.0057	-0.0033
45000	50000	0.3457	0.0063	0.0021	0.0052	-0.0029
50000	60000	0.2959	0.0055	0.0016	0.0044	-0.0028
60000	70000	0.2473	0.0044	0.0013	0.0037	-0.0021
70000	80000	0.2093	0.0038	0.0012	0.0031	-0.0018
80000	90000	0.1915	0.0040	0.0017	0.0029	-0.0022

Table 4 Average capture cross section for $^{238}U(n.\gamma)$ together with the full covariance information based on the AGS concept.

4 Gamma-ray production cross section data

There is a need for a reference cross section for use in γ-ray production cross section measurements. The simplest option is a reference cross section in which a discrete γ-ray is detected, such as the cross section for γ-rays emitted in (n,n'γ) and (n,2nγ) reactions. In the past inelastic scattering of neutrons on ^{56}Fe and ^{52}Cr were considered. However, their inherent limitations imply that other cross sections should be investigated. A number of options have been considered, and neutron reactions on ^{7}Li and ^{nat}Ti have been identified as the best candidates [10], [11].

This report describes briefly the results of cross section measurements for the ^{7}Li(n,n'γ) and ^{nat}Ti(n,n'γ) reactions that have been performed recently at EC-JRC Geel. The experiments were performed with the GAINS γ-ray spectrometer [11], which was installed at a 100 m and 200 m measurement station of the GELINA facility [3]. The GAINS spectrometer consists of 12 HPGe detectors placed at three different angles (110°, 125°, 150°). The incident neutron flux was measurement with a ^{235}U parallel plate fission chamber, which was connected to an analog electronics chain. The data acquisition system for the HPGe detectors uses Acquiris DC440 digitizers, which have a 12-bit amplitude resolution and a sampling rate of 440 million samples/s. The time resolution of the GAINS setup is approximately 10 ns. Absolute efficiency calibration of the GAINS spectrometer is achieved by a combination of measurements with a point-like calibration source and Monte Carlo simulations.

The primary results are the differential γ-production cross sections at the angles mentioned above. The integrated γ-production cross sections are obtained using a standard procedure based on a combination of the Gaussian Quadrature Method and the Legendre Polynomials series expansion of the differential cross sections. More details about the experimental setup and the data analysis procedure are provided in [11], [13], [14] and references therein.

4.1 Cross section data for ^{7}Li(n,n'γ)

M. Nyman, F. Belloni, D. Ichinkhorloo*, E. Pirovano, A.J.M. Plompen, C. Rouki
*Meme Media Laboratory, Hokkaido University, Sapporo 060-8628, Japan

The 477.6-keV $1/2^{-} \rightarrow 3/2^{-}_{g.s.}$ transition in ^{7}Li is one of the best candidates for a reference cross section. There are several factors in favour of this: isotropic γ-ray emission, negligible internal conversion coefficient, low inelastic threshold energy (546 keV), and fairly smooth energy dependence of the cross section. Lithium is also readily available as lithium fluoride (LiF) optical windows. Lithium and beryllium fluorides are also of interest as coolants for Molten Salt Reactor Systems [15][9]. Furthermore, in deuterium-tritium fusion reactors the fuel cycle requires breeding of tritium from ^{6,7}Li. The interactions between neutrons and lithium affect the tritium breeding ratio, nuclear heating, and radiation damage. Thus good quality nuclear data on neutron- and proton-induced reactions of ^{6,7}Li are necessary.

Two experiments were carried out at EC-JRC Geel in 2015. The results of these measurements have been published in [13]. For the first experiment GAINS was situated at the GELINA flight path 3, the sample position being 198.757(5) meters away from the neutron source. In May 2015 the setup was repositioned at the same flight path with the sample at a 99.676(5) m distance. The HPGe detectors were installed in a new support frame, maintaining the same geometry and without changing any of the associated electronics. These data will be referred to as the 200-m and 100-m measurements. For a 200-m flight path the 10 ns time resolution corresponds to a neutron energy resolution of 1.4 keV for E_n = 1 MeV, increasing to 44 keV for E_n = 10 MeV. The sample was an optical-quality lithium fluoride disk of 79.971(1) diameter and 2.05(1) mm thickness. The abundance of ^{7}Li in natural lithium is 92.41(4)% [16]. Integrating the differential cross sections is particularly simple in this case as the γ-ray emission is isotropic: the differential cross section from any given detector needs only to be multiplied by a factor of 4π to obtain the total γ-ray production cross section.

The γ-ray production cross sections for the ^{7}Li(n,$n'\gamma$) reaction obtained from the 200-m and 100-m measurements are displayed in Figure 1. Both data sets meet the goal of the total relative uncertainty being less than 5%. With 1 MeV < E_n < 8 MeV, the average relative uncertainty is approximately 4.5% for both experiments. The main components of the total uncertainty are the HPGe detector efficiency calibration, the fission chamber efficiency, the ^{235}U(n,F) cross section, and statistical uncertainties of the γ-ray and fission chamber yields. As can be seen from the figure, there are significant discrepancies between our data and previous experiments. As different methods for beam monitoring have been used, the possibility of systematic errors is obvious. In order to verify our results, an experiment to measure the ^{7}Li(n,$n'\gamma$) reaction cross section using a different experimental setup will be performed at the nELBE facility in the Helmholtz-Zentrum Dresden-Rossendorf (HZDR) in November 2016.

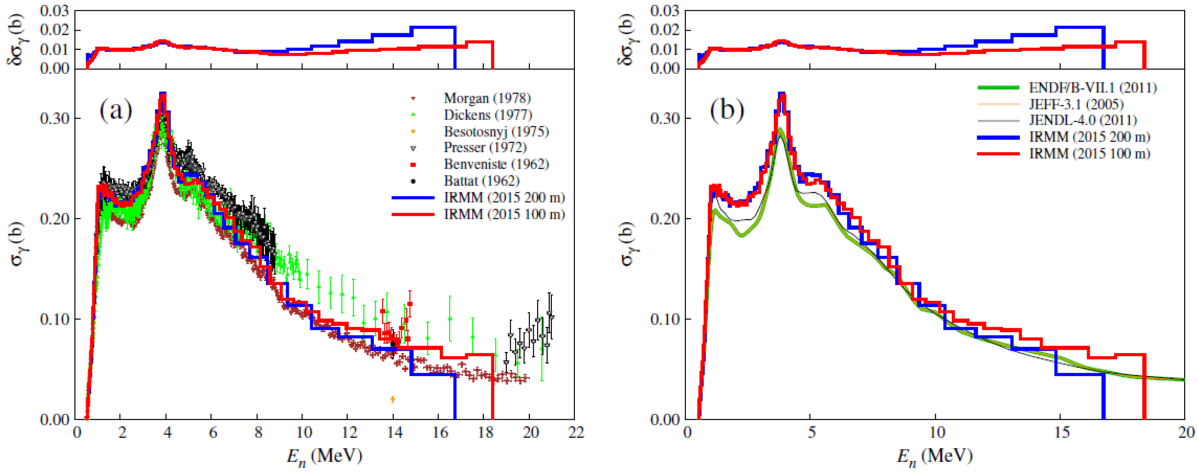

Figure 1 (a) The γ-ray production cross section (σ_γ) for the 477.6-keV transition in ^{7}Li compared with previous experimental data. (b) Our measurements compared with the evaluated cross sections from the ENDF/B-VII.1, JEFF-3.1, and JENDL-4.0 libraries. The total experimental uncertainties ($\delta\sigma_\gamma$) are displayed in the top panels.

4.2 Cross section data for ^{48}Ti(n,n'γ)

A. Olacel*, F. Belloni, C. Borcea*, A. Negret*, M. Nyman, E. Pirovano, A. J. M. Plompen
*Horia Hulubei National Institute for Physics and Nuclear Engineering, Reactorului 30, 077125 Bucharest-Măgurele, Romania

The sample was a natural titanium disc of 8 cm diameter and 0.45 cm thickness. We used γ-ray spectroscopy techniques to determine absolute neutron inelastic scattering cross sections. These data are of interest for nuclear applications (titanium is a structural material in the nuclear reactors) and also for establishing a standard γ-production cross section for neutron-induced reactions [10]. The γ-rays were detected using the GAINS setup [11]. Using the information from the level scheme of ^{48}Ti [17] we calculated the level population and the total inelastic cross sections based on the feeding and the decay of each level of interest. We mention that the data analysis procedure includes also the following corrections: i) for multiple scattering of neutrons in the target and in the close vicinity of it, ii) for the self-attenuation of the γ rays in the sample and iii) for geometrical effects.

The integrated γ-production cross section for the first transition in ^{48}Ti (E_γ=983.5 keV) together with its total uncertainty is shown in Figure 2. The total relative uncertainty of our integrated γ-production cross section is below 5%. The results obtained at GELINA are compared with the data of Dashdorj et al. [18] and results from theoretical calculations performed using the TALYS 1.8 code [19] (default parameters). Given the fact that our sample contained all the stable isotopes of titanium ($^{46-50}$Ti) and the neutron incident energies were higher than the Q-value of the ^{49}Ti(n,2nγ)^{48}Ti reaction, we also had contributions coming from this channel. This contribution could not be extracted from our experimental data. In this context, for a better comparison, we also plot the sum of the cross sections for the two reaction channels resulting from TALYS calculations. While the TALYS predictions underestimate our experimental results, the data of Dashdorj et al. [18] are in good agreement with our data. The only relevant difference between the two experiments is the composition of the sample (natural vs. highly enriched ^{48}Ti). This reflects in the difference between the values of the two γ-production cross sections starting around E_n=9 MeV, which represents the minimum incident neutron energy allowing the excitation of the first level in ^{48}Ti through (n, 2nγ) reactions on ^{49}Ti.

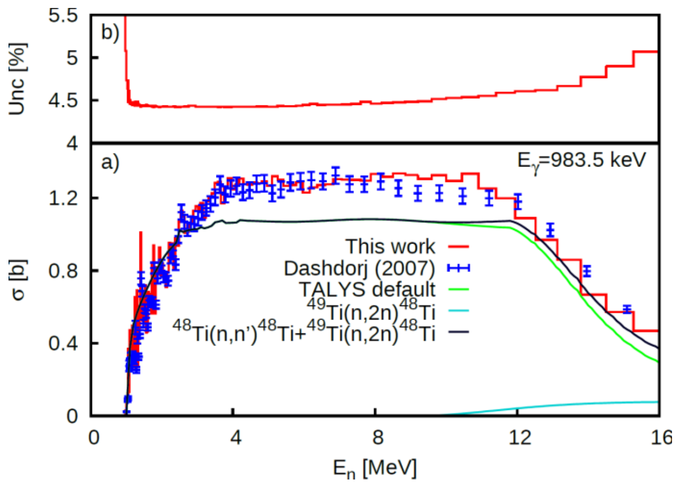

Figure 2 The integrated γ-production cross section of the 983.5 keV transition in ^{48}Ti (a) together with its uncertainty b). The results obtained at GELINA (red line) are compared with other experimental data (in blue) and theoretical calculations using THALYS.

5 Conclusion

High resolution cross section measurements for the $^{7}Li(n,n'\gamma)$, $^{10}B(n,\alpha_0)$, $^{10}B(n,\alpha_1)$, $^{48}Ti(n,n'\gamma)$, $^{197}Au(n,\gamma)$ and $^{238}U(n,\gamma)$ reactions have been carried out at the TOF-facility GELINA. The data have a high accuracy and agree with most of high quality data that are reported in the literature. Most of the experimental details and data reduction and analysis procedures have already been reported in papers published in a refereed journal. The data have been formatted and submitted to the Nuclear Data Section (NDS) of the IAEA such that they can be stored in the EXFOR data library and included a new evaluation of neutron cross section standards which will be finalised by the end of 2016.

References

[1] A.D. Carlson, V.G. Pronyaev, D.L. Smith, N.M. Larson, Z. Chen, G.M. Hale, F.-J. Hambsch, E.V. Gai, Soo-Youl Oh, S.A. Badikov, T. Kawano, H. M. Hofman, H. Vonach, S. Tagesen, "International Evaluation of Neutron Cross Section Standards", Nuclear Data Sheets 110 (2009) 3215 – 3324.

[2] V.G. Pronyaev, A.D. Carlson, R. Capote Noy, "Current Status of Neutron Standards, Summary report of the Technical Meeting", IAEA Headquarters, Vienna, Austria, 1–5 December 2014, INDC(NDS)-0677 (2015).

[3] W. Mondelaers and P. Schillebeeckx,"GELINA, a neutron time-of-flight facility for neutron data measurements", Notiziario Neutroni e Luce di Sincrotrone 11 (2006) 19 – 25.

[4] F.-J. Hambsch and I. Ruskov. "The $^{10}B(n.\alpha_0)$ / $^{10}B(n.\alpha_1\gamma)$ Branching Ratio", Nuclear Science and Engineering 156 (2007) 103 – 114.

[5] P. Schillebeeckx, B. Becker,Y. Danon, K. Guber, H. Harada, J. Heyse, A.R. Junghans, S. Kopecky, C. Massimi, M.C. Moxon, N. Otuka, I. Sirakov and K. Volev, "Determination of resonance parameters and their covariances from neutron induced reaction cross section data", Nuclear Data Sheets 113 (2012) 3054 – 3100.

[6] C. Massimi, B. Becker, E. Dupont, S. Kopecky, C. Lampoudis, R. Massarczyk, M. Moxon, V. Pronyaev, P. Schillebeeckx, I. Sirakov and R. Wynants, "Neutron capture cross section measurements for ^{197}Au from 3.5 keV to 85 keV at GELINA", European Physics Journal A 50 (2014) 124, 1 – 12.

[7] H.I. Kim, C. Paradela, I. Sirakov, B. Becker, R. Capote, F. Gunsing, G.N. Kim, S. Kopecky, C. Lampoudis, Y.-O. Lee, R. Massarczyk, A. Moens, M.. Moxon, V.G. Pronyaev, P. Schillebeeckx and R. Wynants, "Neutron capture cross section measurements for ^{238}U in the resonance region at GELINA", European Physics Journal A 52 (2016) 170, 1 – 20.

[8] G. Giorginis and V. Khriatchkov, "The effect of particle leaking and its implications for measurements of the (n,α) reaction on light elements by using ionisation chambers", Nuclear Instruments and Methods in Physics Research, Section A: Accelerators, Spectrometers, Detectors and Associated Equipment 538 (2005) 550 – 558.

[9] B. Becker, C. Bastian, F. Emiliani, F. Gunsing, J. Heyse, K. Kauwenberghs, S. Kopecky, C. Lampoudis, C. Massimi, N. Otuka, P. Schillebeeckx and I. Sirakov, "Data reduction and uncertainty propagation of time-of-flight spectra with AGS", J. of Instrumentation, 7 (2012) P11002, 1– 19.

[10] A.D. Carlson, V.G. Pronyaev, F.-J. Hambsch, W. Mannhart, A. Mengoni, R.O. Nelson, P. Talou, S. Tagesen and H. Vonach, "An update of the nuclear data standards activities", Journal of the Korean Physical Society 59 (2011) 1390-1395.

[11] A.D. Carlson, V.G. Pronyaev, R. Capote, F.-J. Hambsch, F. Käppeler, C. Lederer, W. Mannhart, A. Mengoni, R.O. Nelson, A.J.M. Plompen, P. Schillebeeckx, S. Simakov, P. Talou, S. Tagesen, H. Vonach, A. Vorobyev and A. Wallner, "Imrpovements and Extensions of the Neutron Cross Section and Fluence Standards", Nuclear Data Sheets 118 (2014) 126 – 131.

[12] D. Deleanu, C. Borcea, Ph. Dessagne, M. Kerveno, A. Negret, A.J.M. Plompen and J. C. Thiry, "The gamma efficiency of the GAINS spectrometer", Nuclear Instruments and Methods in Physics Research, Section A: Accelerators, Spectrometers, Detectors and Associated Equipment 624 (2010) 130 – 136.

[13] M. Nyman, F. Belloni, D. Ichinkhorloo, E. Pirovano, A.J.M. Plompen, and C. Rouki, "Measurement of the 477.6-keV γ-ray production cross section following inelastic neutron scattering by ^{7}Li", Physical Review C 93 (2016) 024610 .

[14] Adina Olacel, "Neutron cross section measurements and Monte Carlo simulations of gamma spectroscopy setups", Ph.D. thesis, Faculty of Physics, University of Bucharest (2016).

[15] U.S. DOE Nuclear Energy Research Advisory Committee and the Generation IV International Forum (GIF): "A Technology Roadmap for Generation IV Nuclear Energy Systems", https://www.gen-4.org/gif/jcms/c_9260/public, (2002).

[16] K.J.R. Rosman and P.D.P. Taylor, "Isotopic Compositions of the Elements 1997", Pure and Applied Chemistry 70, 217 (1998).

[17] T. W. Burrows, "Nuclear Data Sheets for A = 48", Nuclear Data Sheets 107 (2006) 1747 – 1922.

[18] D. Dashdorj, G. E. Mitchell, J. A. Becker, U. Agvaanluvsan, L. A. Bernstein, W. Younes, P. E. Garrett, M. B. Chadwick, M. Devlin, N. Fotiades, T. Kawano and R. O. Nelson, "Gamma-Ray Production Cross Sections in Multiple Channels for Neutron-Induced Reaction on ^{48}Ti for E_n = 1 to 200 MeV", Nuclear Science and Engineering 157 (2007) 65 – 77.

[19] A. J. Koning, S. Hilaire and M. C. Duijvestijn, "TALYS-1.0", International Conference on Nuclear Data for Science and Technology, April 22-27, 2007, Nice, France, editors O. Bersillon, F. Gunsing, E. Bauge, R. Jacqmin, and S. Leray, EDP Sciences, 211 – 214.

List of abbreviations and definitions

CSWEG	Cross Section Evaluation Working Group
EC	European Commission
GAINS	Gamma Array for Inelastic Neutron Scattering
GELINA	Geel Electron LINear Accelerator
IAEA	International Atomic Energy Agency
JRC	Joint Research Centre
NDS	Nuclear Data Section
OECD	Organisation for Economic Co-operation and Development
PMT	PhotoMultiPlier
TFGIC	Twin Frisch-Grid Ionisation Chamber
TOF	Time-Of-Flight
WPEC	Working Party on international Evaluation Cooperation

List of figures

Figure 1 (a) The γ-ray production cross section (σ_γ) for the 477.6-keV transition in ^{7}Li compared with previous experimental data. (b) Our measurements compared with the evaluated cross sections from the ENDF/B-VII.1, JEFF-3.1, and JENDL-4.0 libraries. The total experimental uncertainties ($\delta\sigma_\gamma$) are displayed in the top panels........................ 10

Figure 2 The integrated γ-production cross section of the 983.5 keV transition in ^{48}Ti (a) together with its uncertainty b). The results obtained at GELINA (red line) are compared with other experimental data (in blue) and theoretical calculations using THALYS........ 11

List of tables

Table 1 Parameters of the Legendre polynomials for the α_0 channel. 4

Table 2 Parameters of the Legendre polynomials for the α_1 channel 5

Table 3 Average capture cross section for ^{197}Au(n.γ) together with the full covariance information based on the AGS concept. 7

Table 4 Average capture cross section for ^{238}U(n.γ) together with the full covariance information based on the AGS concept. 8

LC-NA-28161-EN-N

JRC Mission

As the Commission's
in-house science service,
the Joint Research Centre's
mission is to provide EU
policies with independent,
evidence-based scientific
and technical support
throughout the whole
policy cycle.

Working in close
cooperation with policy
Directorates-General,
the JRC addresses key
societal challenges while
stimulating innovation
through developing
new methods, tools
and standards, and sharing
its know-how with
the Member States,
the scientific community
and international partners.

Serving society
Stimulating innovation
Supporting legislation

Publications Office

doi:10.2789/306587

ISBN 978-92-79-62864-1